Lakes_cci - Algorithm Development Plan (ADP)

Reference CCI-LAKES2-0014-ADP

Issue 3.0.0 – 7/10/2025

Contract number : 4000125030/18/I-NB –Lakes_cci

For internal use

11 rue Hermès, Parc Technologique du Canal — 31520 Ramonville Saint-Agne, France
Tel +33 (0)5 61 39 47 00 Fax +33(0)5 61 75 10 14
www.cls.fr

CHRONOLOGY OF ISSUES

Issue	Legacy Issues	Date	Objective	Written by
1.0	1.0	19/03/2020	Initial Version	S. Simis, JF Crétaux, H Yésou, E Malnes, H Vickers, P Blanco, C Merchant, L Carrea, C Duguay, Y Wu
	1.1	24/04/2020	Revision following ESA review	See above
	2.0	30/07/2020	LSWT MODIS data processing	C Merchant
	2.1	29/09/2020	Revision following ESA review	JF Crétaux, C Merchant, H Yésou, E Malnes
2.x	2.2	02/05/2022	Updates accompanying CRDP v2.0 and v2.0.1	X Liu, JF Crétaux, L Carrea, C Duguay, S Simis
	2.3	06/07/2022	Revision following ESA review	B. Calmettes
2.1	-	06/09/2023	Revision and updates accompanying CRDP v2.1.0, outlook towards CRDP v3.0.0	S. Simis, B Calmettes, JF Crétaux, X Liu, A Mangili, H Yésou, L Carrea, C Duguay, Y Wu
2.1.1		17/10/2023	Revision following ESA review	S. Simis, B Calmettes, JF Crétaux, X Liu, A Mangili, H Yésou, L Carrea, C Duguay, Y Wu
3.0.0	-	07/10/2025	Documentation accompanying CRDP v3.0.0	S. Simis, B Calmettes, JF Crétaux, X Liu, A Mangili, H Yésou, L Carrea, C Duguay, Y Wu

Note: prior to document issue 2.1, the PVASR and ADP were provided in a combined document. From v2.1 onwards the two documents are provided separately and versioning is kept consistent with the CRDP release cycle.

BIBLIOGRAPHIC REFERENCE

This document is only intended for internal use.

DOCUMENT REVIEW

Checked by	Stefan Simis – PML J-F Cretaux - LEGOS	S. Simis
Approved by	Philippe Mourot - CLS	Pmourot
Authorized by	Clément Albergel - ESA	clement.albergel

LIST OF CONTENTS

1 Introduction

The ADP details for each Lakes_cci ECV product:

- Algorithm developments planned to feature in CRPD v3.0. Examples include updates to models, classification codes, and algorithm training or calibration, at any processing level.
- Priorities for future algorithm developments beyond the next annual cycle.

For LWE, LWLR, LSWT, LIC and LIT products, the existing validation and identified issues are reported in the Product Validation and Algorithm Selection report (PVASR v3.0.0) and not repeated here.

This Algorithm Development Plan (ADP) is not intended for public distribution.

2 Lake Water level - LWL

2.1 Candidate algorithms for LWL

Two algorithms have been developed at LEGOS for the calculation of the LWL, with details provided in the ATBD.

The first one is incorporated in the Hysope code and is operated at CLS in the framework of the Hydroweb database. A version for non-operational use also runs at LEGOS and is based on the same equations but using Geophysical Data Records (GDRs, delivery delay = 90 days) instead of IGDRs (delivery delay 1 to 2 days, Cretaux et al., 2016). The second algorithm, Lakes Physical Processor (LPP, Boy et al 2022) is operated at LEGOS. The main difference between the two algorithms is that the first algorithm uses the value of the range provided in the IGDR files (generated by agencies) while the LPP estimates the range base on simulation of the waveform (Crétaux et al 2009, Boy et al 2022).

The procedure is run against data within a priori defined polygons of lake contours (using the common dataset of maximum water extent outlines created for Lakes_cci) which are then processed using the Hysope software which is classically using the following equation:

$$LWL = Alt - R_{corr} - TE \qquad [2.1]$$

Where LWL is considered with respect to a geoid, R_{corr} is the measured range between the satellite and the lake surface, *Alt* is the altitude of the satellite above an ellipsoid and TE is the combination of all correction factors to take into account atmospheric refraction (propagation in the ionosphere and the troposphere), tidal effects (solid Earth, lake and polar), and geoid height above the ellipsoid. For detailed information a full discussion of the computation of LWL is found in Cretaux et al. (2009).

All corrections are released in the GDRs or the IGDRs. The range is chosen from different retracking considering that generally the OCOG retracking is the most suitable for continental surface (see E3UB). The geoid correction is calculated using the repeat track technique (see E3UB and Cretaux et al. 2009, 2016).

2.2 Validation results for LWL

The algorithm used to calculate water level over lakes is well established in scientific literature. To address the issues that are listed in the following sections, we need to analyse lakes where reference in situ data are available. Examples of these procedures are given in Ricko et al. (2012) and Arsen et al. (2015), comparing different lake databases.

Lakes_cci cooperates with the State Hydrological Institute of St Petersburg, which provides in situ data of LWL for a set of Russian and central Asian lakes. We also use existing databases on the web to increase the number of lakes that can be used for this purpose.

The comparative analysis allows the statistically best performing retracking algorithm to be selected, as has been widely demonstrated for lakes as well as rivers.

Additional metrics to validate the LWL products include comparison of individual LWL retrieval to the long-term LWL variability, to detect outliers. The impact of removing outliers is traced as part of this process.

2.3 Identified issues for LWL

There are two main issues currently under investigation for the processing of altimetry data over lakes. The first is related to the onboard tracking system, and the second is related to the processing of altimetry over small lakes.

We have identified solutions to address onboard tracking issues based on new a priori information. For retrieval of LWL over small lakes we identify solutions based in new algorithms for SAR data. Both approaches are detailed in section 2.4.

Another separate consideration of retrieval performance is the calculation of relative biases when several satellites of different types of orbits are used over a given lake. When we use a series of satellites such as Topex / Poseidon, Jason-1/2/3, Sentinel-6A, we collect data from the same orbit, so that the relative bias between each mission is well described and calibrated (see Cretaux et al. 2009, 2011, 2013, 2018, Bonnefond et al. 2018). When observations from different orbit are used, however, such as with Jason and Envisat or Jason and Sentinel-3, another bias is added. The instrumental biases are known, but since the tracks do not cover the same position over the lake, an additional bias due to geoid error must be considered. A very simple method was developed at LEGOS to correct for this additional bias. The LWL is calculated independently using each track, over the whole period, and during the overlapping period we interpolate the point measurement from each pass and calculate the average difference between all interpolate points. It then corresponds to the additional bias due to geoid errors.

2.4 Future improvements for LWL

In previous versions of the ADP we have proposed to use results from the FDR4ALT project and LPP approach. Data from FDR4ALT (Envisat) was already used in lakes_cci V2.1 and LPP is implemented in the processing chain since 2024. For CRDP v3.0.0, we will include results from these two approaches where necessary: FDR4ALT when ENVISAT is used, and LPP for small lakes with the SAR data on Sentinel-3A, 3B and Sentinel-6.

2.5 LWL References

Arsen, A., JF. Cretaux, and R. Abarca-Del-Rio. 2015. Use of SARAL/AltiKa over mountainous lakes, intercomparison with Envisat mission J. of Adv. Space Res. The Saral/ALtiKa satellite Altimetry Mission, 38, 534-548, 2015, doi: 10. 1080/01490419. 2014. 1002590

Bonnefond, P. ; Verron, J. ; Aublanc, J. ; Babu, K. N. ; Berge-Nguyen, M. ; Cancet, M. ; Chaudhary, A. ; Cretaux, J-F. ; Frappart, F. ; Haines, BJ. , Laurain, O. ; Ollivier, A. ; Poisson, JC. ; Prandi, P. ; Sharma, R. ; Thibaut, P. ; Watson, C. The benefits of the Ka-Band as evidenced from the SARAL/AltiKa Altimetric mission: quality assessment and unique characteristics of AltiKa data, Remote Sensing. 2018, 10(1), 83, doi:1039/rs/10010083

Boy F., Cretaux J-F., Boussaroque M., & Tison C., 2022, Improving Sentinel-3 SAR mode procesisng over lake using numérical simulations, IEEE Transactions on Geoscience and Remote Sensing, 60, 1-18, Art no. 5220518, doi: 10.1109/TGRS.2021.3137034

Cretaux, J. F., S. Calmant, V. Romanovski, et al. 2009. An absolute calibration site for radar altimeters in the continental domain: lake Issykkul in Central Asia, Journal of Geodesy 83 (8) 723-735 DOI: 10. 1007/s00190-008-0289-7

Cretaux, J. F., S. Calmant, V. Romanovski, et al. 2011 Absolute Calibration of Jason radar altimeters from GPS kinematic campaigns over Lake Issykkul, Marine Geodesy, 34 : 3-4, 291-318, DOI: 10. 1080/01490419. 2011. 585110

Crétaux J-F., Bergé-Nguyen M., Calmant S., Romanovski V. V., Meyssignac B., Perosanz F., Tashbaeva S., Arsen A., Fund F., Martignago N., Bonnefond P., Laurain O., Morrow R., Maisongrande P., 2013 Calibration of envisat radar altimeter over Lake Issykkul, J. Adv. Space Res., Vol 51, 8, 1523-1541, doi: 10. 1016/j. asr. 2012. 06. 039

Cretaux J-F, M. Bergé-Nguyen, S. Calmant, N. Jamangulova, R. Satylkanov, F. Lyard, F. Perosanz, J. Verron, A. S. Montazem, G. Leguilcher, D. Leroux, J. Barrie, P. Maisongrande and P. Bonnefond,

2018, Absolute calibration / validation of the altimeters on Sentinel-3A and Jason-3 over the lake Issykkul, Remote sensing, 10, 1679, ; doi:10. 3390/rs10111679

Egido A., and W. H. F Smith, 2017, Fully Focused SAR altimetry: Theory and Applications, IEEE, 55, 1

Ričko M., C. M. Birkett, J. A. Carton, and J-F. Cretaux, Intercomparison and validation of continental water level products derived from satellite radar altimetry, J. of Applied Rem. Sensing, Volume 6, Art N°: 061710, DOI: 10. 1117/1. JRS. 6. 061710, 2012

3 Lake water extent - LWE

3.1 Candidate algorithms for LWE

Based on inter-comparison on a small set of lakes with increasingly complex hydromorphology, an approach based only on optical HR imagery was previously adopted to generate the LWE product. Water surfaces are extracted from images based on the exploitation of an in-house processing chain (Figure 1), named ExtractEO (Maxant et al, 2022). This software suite is also in use for Copernicus EMS, and for the supply of "water surface" reference plans for SWOT CalVAL globally.

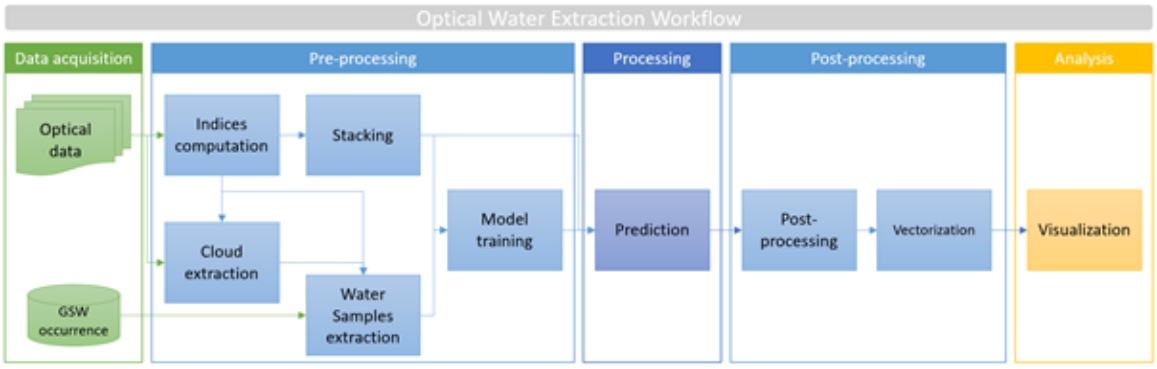

Figure 1: Optical Water Extraction Workflow

The preprocessing steps correspond to:

- Region Of Interest (ROI) is defined including the target lake.
- Selection of set of images representative of the different water levels of the target.
- Indices generation 'AWEI, NDWI, MNDWI, NDI, SWIS which is a combination of indices)

The processing then follows the scheme shown in Figure 2:

- Automatic water sample generation from Global Surface Water. Water indices are computed to remove outliers and filter the training samples to the hydrological reality of the image (water extent, resolution)
- Training using the Multi-Layer Perceptron classifier (optionally a Support Vector Machine (SVM) or Random Forest (RF) approach can be applied)
- Slope and hillshade thresholds derived from HR DEMs are applied to refine the water extraction (post-processing)
- Minimum mapping unit (MMU) sieving to remove small features (0,1 hectares in this case)
- Water extent (in km^2) is subsequently calculated using the sum of individual pixel classified as water pixel within the ROI
- Generation of a max extent water mask

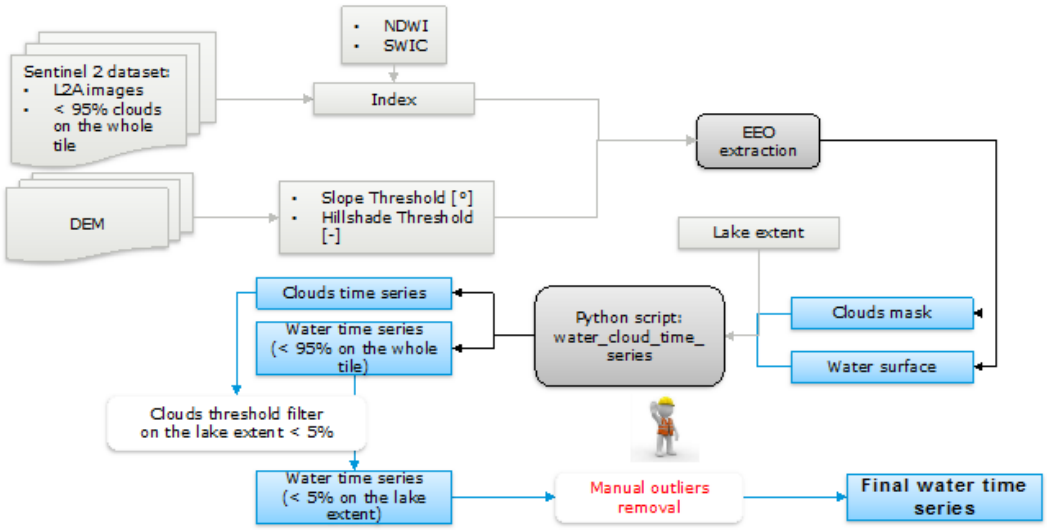

Figure 2: Detailed workflow of the water extraction procedure within ExtractEO

3.2 Future improvements for LWE

The method using SVM on optical imagery appears to provide a reliable and consistent approach despite sensitivity to cloud cover, and to a lesser degree, sunglint.

The presence of sunglint on water surfaces can disrupt the process of recognising and extracting water bodies (Gao et la., 2023). The appearance of this phenomenon depends not only on the position of the sun, but also on the location of the target in the swath. To limit re-treatments (Harmel et al., 2018; Tavares et al., 2021) it would be beneficial to develop a sunglint flag. This would allow automatic adjustment of relevant coefficients and thresholds in the ExtractEO processing chain.

Concerning cloud coverage, refinement of the existing cloud detector in the ExtractEO chain to provide a better cloud detection on the S2 L2A product, would be beneficial. This could be based in Machine Learning. The improved detection of clouds mask could be compared furthermore with such ancillary data as the SAFE mask from Colorado Boulder University or the Idepix procedure used within LWLR product generation. To address (small) cloud gaps, common water occurrence maps in databases such as GWS (Pekel et al. 2016) or GLAD (Pickens et al., 2022) might prove useful. Concerning cloud masks, the Maja process handled by CNES to generate level 2 Sentinel 2 products, would be upgraded in 2025, ^providing more spatially defined cloud mask, ie 20 m for 400m actually, and this with an improved accuracy.

3.3 LWE References

Gao B-C, Li R-R. 2323. A Multi-Band Atmospheric Correction Algorithm for Deriving Water Leaving Reflectances over Turbid Waters from VIIRS Data. Remote Sensing. 2023; 15(2):425. https://doi.org/10.3390/rs15020425

Harmel T., Chami M., Tormos Th, Reynaud N., Danis P.A., 2018.Sunglint correction of the Multi-Spectral Instrument (MSI)-SENTINEL-2 imagery over inland and sea waters from SWIR bands, Remote Sensing of Environment, 204, 308-321, https://doi.org/10.1016/j.rse.2017.10.022.

Maxant J, Braun R, Caspard M, Clandillon S. (2022). ExtractEO, a Pipeline for Disaster Extent Mapping in the Context of Emergency Management. Remote Sensing. .14(20):5253. https://doi.org/10.3390/rs14205253

Pekel JF, Cottam A, Gorelick N, Belward AS. 2016.High-resolution mapping of global surface water and its long-term changes. Nature. 2016 Dec 15;540(7633):418-422. doi: 10.1038/nature20584.

Pickens, A.H., Hansen, M.C., Stehman, S.V., Tyukavina, A., Potapov, P., Zalles, V., Higgins, J. (2022) Global seasonal dynamics of inland water and ice. Remote Sensing of Environment, Volume 272, 112963

Tavares M.H., Lins R.C., Harmel T., Fragoso C.R. Jr., Martínez J.M., Motta-Marques D.,2021. Atmospheric and sunglint correction for retrieving chlorophyll-a in a productive tropical estuarine-lagoon system using Sentinel-2 MSI imagery, ISPRS Journal of Photogrammetry and Remote Sensing, 174, 215-236, https://doi.org/10.1016/j.isprsjprs.2021.01.021.

4 Lake surface water temperature - LSWT

4.1 Candidate algorithms for LSWT

Surface temperatures from infrared observations are obtained by coefficient-based methods or optimal estimation (OE, Merchant and Embury 2014). Because of the varied altitudes of lakes and the large differences in atmospheric absorption associated with continentality, optimal estimation is the appropriate approach for LSWT estimation (MacCallum and Merchant, 2012).

OE also provides comprehensive equations for uncertainty evaluation, on which basis uncertainty estimates are provided in LSWT products per datum.

As well as retrieval, classification of which pixels are filled with water under clear skies is a necessary part of the LSWT processing. This is done by a “fuzzy logic” style approach in which several metrics with fuzzy thresholds are combined into a “water detection score” that contributes to the definition of the quality level attributed to the pixel. Bayesian cloud detection, as used for sea surface temperature, was also considered to identify clear-sky pixels but is heavily compromised in its current implementation for small lakes, where the spatial coherence of the temperature of the scene is not a good indicator of cloud (unlike in the centre of large lakes and over open ocean). Because of the user requirement to increase the number of measured lakes, the latter scheme is therefore currently inapplicable for the identification of clear-sky only water pixels.

4.2 Future improvements for LSWT

For CRDP v3.1 (LSWT v5.0, the following improvements are considered:

1. Inter-sensor consistency: The CDR is made from seven sensors (2 ATSRs, MODIS, 2 AVHRRs and 2 SLSTRs) which have similar channels and nadir spatial resolution. Biases between sensor observations of a given lake arise because of relative calibration errors between sensors. New for v3.1 is that calibration adjustments are applied to brightness temperature. We are able to take advantage of bias-aware optimal estimation parameters obtained for AVHRRs within SST CCI (using plentiful ocean in situ data as an in-flight calibration reference). While not tuned for lakes, these will nonetheless reduce over-lake calibration biases.
2. Including night-time observations: This is a high-risk high-reward objective given the number of sensors, the subtlety required for nighttime detection of clouds, and the small amount of funded effort for the attempt. Nonetheless, Bayesian cloud detection (adapted again from SST CCI) is applied on nighttime observations, based on a new climatology of LSWT from CDRP v2.1. In case validation of the nighttime results justifies their inclusion in v3.1, this approximately doubles the observation frequency for some lakes (not necessarily all).
3. LSWT v5.0 will use ERA-5 for background numerical weather prediction information (except the lake surface water temperature which will be the climatology from CDR v2.1) and uses RTTOV12.

Beyond LSWT v5.0:

1. TRISHNA, which is planned to be launched in 2026, will offer measurements that are unique for LSWT coverage, quality and especially resolution, allowing to retrieve LSWT for smaller lakes with a higher frequency than the current high-resolution instruments which have low revisiting time (more than 15 days).
2. Landsat collection 6 reprocessing. Despite the long revisiting time (>15days), given the high resolution, Landsat can offer an increased number of observations. This is critical for lakes in certain regions such as Greenland where lakes are typically small for the 1km resolution instruments such SLSTR, AVHRR etc... Furthermore, Landsat can offer a long-time coverage providing long time series of high-resolution measurements creating an archive of historical data which can benefit/complement data from the new upcoming high-resolution sensor such as TRISHNA.

3. The U. S. successor to MODIS and AVHRR is the VIIRS series, providing excellent LSWT coverage and quality. Selected VIIRS data will be available at CEDA and therefore it would be interesting to attempt to retrieve LSWT from VIIRS which offers a better resolution (750m) than the classic meteorological satellites.
4. The SGLI instrument on the JAXA satellite GCOM-C has been launched in 2017 and produce observations in the thermal infrared band at 500m spatial resolution (although 250m seems to be also available) with a revisiting time of 2 days. It could be useful to retrieve LSWT for smaller lakes. However, the 3.7-micron channel is not available and therefore LSWT can be retrieved during daytime only since the 3.7 channel is critical for Bayesian cloud detection during nighttime.
5. Rivers. Given the increasing quality and availability of high spatial resolution thermal infrared sensors, the retrieval of water temperature in rivers is becoming more feasible. The monitoring of fresh water and heat discharge through rivers is critical for example in the Arctic for the elucidation of the quantitative role of the Arctic rivers in the recently rapidly changing Arctic climate system. Meteorological data analysis and especially in situ data are generally not sufficient. In situ data are point measurements and often at very low temporal resolution especially in remote regions such as the Arctic.
6. Lakes that are drying up (or expanding): especially with high resolution sensors it could be beneficial to utilise a dynamic mask rather than a static mask to allow LSWT to be retrieved for water area larger than the area covered by the static mask.
7. The gap-filled LSWT can be a good prior and can be used instead of the LSWT climatology, currently used for the OE retrieval. This will offer improvements in the retrieval but especially in the Bayesian cloud detection. This will help to improve the cloud detection during nighttime but also daytime cloud detection could be attempted. Therefore, future improvements could be aimed at improving the cloud/water detection.

5 Lake water leaving reflectance - LWLR

5.1 Candidate algorithms for LWLR

Significant progress has been made in recent years on water quality estimation algorithms, largely prompted by the operational delivery of OLCI (Ocean and Land Colour Instrument) data. New algorithms, ranging from machine-learning-based to semi-analytical and empirical approaches, have been developed. However, there remains a crucial need for an independent validation of water quality algorithms specifically designed for the OLCI sensor. In many cases, the same algorithms can still be applied to the Medium Resolution Imaging Sensors (MERIS), which was the focus of the previous algorithm selection and tuning exercise for sensors with this waveband set. For MODIS-Aqua, the first algorithm selection and tuning exercise was completed for the previous version (2.x) of the Lakes_cci CRDP.

With CRDPv3.0, an upgrade to the atmospheric correction code (Polymer v4.17) is applied to data from MERIS, MODIS-Aqua and OLCI. This has prompted the need to re-evaluate algorithm selection and calibraton for each of the Optical Water Types (OWT) recognised in the Lakes_cci, and subsequent remapping of best-performing algorithms as input to the OWT-blended outputs. Details of these procedures are provided in the ATBD.

The comprehensive algorithm calibration and validation involves the inclusion of previous candidate algorithms and thus including those previously selected and implemented in Lakes_cci v2.x. For OLCI, additional algorithms published in recent years are evaluated. A summary of the candidate algorithms for chlorophyll-a (Chla) and Total Suspended Matter (TSM) relating to OLCI is given in Table 1.

The upgrades to the atmospheric correction software used to produce LWLR necessitate recalibration of algorithms regardless of the instrument that is used. The impact of these changes is expected to be minor for clear lakes but larger with turbid and productive lakes, due to the nature of changes in the atmospheric correction code. New candidate algorithms could also be introduced for MODIS by adjusting the corresponding OLCI bands to the nearest MODIS bands where available. As a result of these updates, additional lakes may be found to provide meaningful results beyond the previous selection of 48 relatively large lakes. Similarly, whilst TSM products could not be successfully formulated for MODIS in the previous production cycle, the atmospheric correctoin improvements may see improvement here.

Table 1: Summary of candidate new Chla algorithms for OLCI

Algorithm	Architectural approach	Formular	Original training (mg.m-3)	reference
OC4_OLCI	Blue-green ratios	MBR=Rrs(443>490>510)/Rrs560	0.01 to 78	O'Reilly and Werdell 2019
OC5_OLCI	Blue-green ratios	MBR=Rrs(413>443>490>510)/Rrs560	0.01 to 78	O'Reilly and Werdell 2019
OC6_OLCI	Blue-green ratios	MBR=Rrs(413>443>490>510)/M(560&665)	0.01 to 78	O'Reilly and Werdell 2019
OC4_MERIS	Blue-green ratios	MBR=Rrs(442>490>510)/Rrs560	0.01 to 78	O'Reilly and Werdell 2019
OC5_MERIS	Blue-green ratios	MBR=Rrs(412>442>490>510)/Rrs560	0.01 to 78	O'Reilly and Werdell 2019
OC6_MERIS	Blue-green ratios	MBR=Rrs(412>442>490>510)/M(560&665)	0.01 to 78	O'Reilly and Werdell 2019
Optimized QAA for OLCI	Semi-analytical	1 Modified reference band ( ) of 709 or 754 nm in QAA Step 3: If MCI≤0.0016 choose 709 nm, else 754 nm 2 Modified equation and η value in Step 7	5 to 100	Liu et al. 2020

MDN	Machine learning	Mixed Density Network	0.2 to 1209	Pahlevan, Smith et al. 2020, Pahlevan, Smith et al. 2021, Smith, Pahlevan et al. 2021
Bayesian	Bayesian probabilistic neural networks	Bayesian Neural Network	0.05 to 68	Werther et al. 2022
Smith18	Switched blending (G2B, OCI)	G2B algorithm refers to Gilerson, Gitelson et al. (2010). OCI algorithm refers to combined CI (Chl<0.25) and OC4E (Chl>0.25) algorithms.	0.43 to 309	(Smith, Lain et al. 2018)

Table 2: Summary of candidate new Turbidity/TSM algorithms for OLCI

Algorithm	Architectural approach	Formular	Original training (g.m-3)	reference
SOLID20	MDN-based bbp inversion	Classification based	0.1 to 2626.8	Balasubramanian et al. 2020
Jiang21	Semi-analytical	Classification based	0.09 to 2627	Jiang et al. 2021
Novoa21G	Switch blending	Linear-Green (TSM<10), Linear-Red (TSM 10~50), Poly-NIR (TSM>50)	2.6 to 1579.1	Novoa et al. 2017
Novoa21B	Switch blending	Linear-Green (TSM<10), Nechad et al. (2010) NIR (TSM 10~50), Nechad et al. (2010) NIR (TSM>50)	17.8 to 340.6	Novoa et al. 2017
Uudeberg20-clear	Band ratios		0.5 to 215.2	Uudeberg et al. 2020
Uudeberg2020-moderate	Band ratios		0.5 to 215.2	Uudeberg et al. 2020
Uudeberg20-Turbid	Band ratios		0.5 to 215.2	Uudeberg et al. 2020
Uudeberg20-VeryTurbid	Band ratios		0.5 to 215.2	Uudeberg, et al. 2020
Uudeberg20-Brown	Band ratios		0.5 to 215.2	Uudeberg et al. 2020
ANTA21 (Turbidity)	(based on Nechad 2009, tuned for OLCI)	T(red) was used if RW(red) < 0.05, and T(NIR) if RW(red) > 0.07, with a linear blending in the transition. Red=665 nm, NIR=865 nm	0.83 to 176 FNU	Nechad et al. 2009, Dogliotti, et al. 2015, Klein, et al. 2021

*: ATA21 algorithm was developed for Turbidity

5.2 Future improvements for LWLR

LWLR data reprocessing for CRDP v3.0.0 using the upgraded algorithms for LWLR and derived biogeochemical products requires re-analysis of quality flagging and masking procedures, including the cluster-based identification of outlier data under near-freezing conditions.

CDOM algorithms have been proposed for inclusion in CDRP v3.0.0, and have been validated as reported in the *Technical Note: CDOM algorithm development for global inland waters*, available through the

project website. Quality flagging and masking procedures for the CDOM products also remain to be developed for CRDP v3.0.0.

5.3 LWLR References

Balasubramanian, S. V., N. Pahlevan, B. Smith, C. Binding, J. Schalles, H. Loisel, D. Gurlin, S. Greb, K. Alikas and M. Randla (2020). Robust algorithm for estimating total suspended solids (TSS) in inland and nearshore coastal waters. Remote Sensing of Environment **246**: 111768.

Dogliotti, A. I., K. Ruddick, B. Nechad, D. Doxaran and E. Knaeps (2015). A single algorithm to retrieve turbidity from remotely-sensed data in all coastal and estuarine waters. Remote sensing of environment **156**: 157-168.

Gilerson, A. A., A. A. Gitelson, J. Zhou, D. Gurlin, W. Moses, I. Ioannou and S. A. Ahmed (2010). Algorithms for remote estimation of chlorophyll-a in coastal and inland waters using red and near infrared bands. Optics Express **18**(23): 24109-24125.

Jiang, D., B. Matsushita, N. Pahlevan, D. Gurlin, M. K. Lehmann, C. G. Fichot, J. Schalles, H. Loisel, C. Binding and Y. Zhang (2021). Remotely estimating total suspended solids concentration in clear to extremely turbid waters using a novel semi-analytical method. Remote Sensing of Environment **258**: 112386.

Klein, K. P., H. Lantuit, B. Heim, D. Doxaran, B. Juhls, I. Nitze, D. Walch, A. Poste and J. E. Søreide (2021). The Arctic Nearshore Turbidity Algorithm (ANTA)-A multi sensor turbidity algorithm for Arctic nearshore environments. Science of Remote Sensing **4**: 100036.

Liu, G., L. Li, K. Song, Y. Li, H. Lyu, Z. Wen, C. Fang, S. Bi, X. Sun and Z. Wang (2020). An OLCI-based algorithm for semi-empirically partitioning absorption coefficient and estimating chlorophyll a concentration in various turbid case-2 waters. Remote Sensing of Environment **239**: 111648.

Nechad, B., K. Ruddick and G. Neukermans (2009). Calibration and validation of a generic multisensor algorithm for mapping of turbidity in coastal waters. Remote Sensing of the Ocean, Sea Ice, and Large Water Regions 2009, SPIE.

Novoa, S., D. Doxaran, A. Ody, Q. Vanhellemont, V. Lafon, B. Lubac and P. Gernez (2017). Atmospheric corrections and multi-conditional algorithm for multi-sensor remote sensing of suspended particulate matter in low-to-high turbidity levels coastal waters. Remote Sensing **9**(1): 61.

O'Reilly, J. E. and P. J. Werdell (2019). Chlorophyll algorithms for ocean color sensors-OC4, OC5 & OC6. Remote sensing of environment **229**: 32-47.

Pahlevan, N., B. Smith, C. Binding, D. Gurlin, L. Li, M. Bresciani and C. Giardino (2021). Hyperspectral retrievals of phytoplankton absorption and chlorophyll-a in inland and nearshore coastal waters. Remote Sensing of Environment **253**: 112200.

Pahlevan, N., B. Smith, J. Schalles, C. Binding, Z. Cao, R. Ma, K. Alikas, K. Kangro, D. Gurlin and N. Hà (2020). Seamless retrievals of chlorophyll-a from Sentinel-2 (MSI) and Sentinel-3 (OLCI) in inland and coastal waters: A machine-learning approach. Remote Sensing of Environment **240**: 111604.

Smith, B., N. Pahlevan, J. Schalles, S. Ruberg, R. Errera, R. Ma, C. Giardino, M. Bresciani, C. Barbosa and T. Moore (2021). A chlorophyll-a algorithm for Landsat-8 based on mixture density networks. Frontiers in Remote Sensing **1**: 623678.

Smith, M. E., L. R. Lain and S. Bernard (2018). An optimized chlorophyll a switching algorithm for MERIS and OLCI in phytoplankton-dominated waters. Remote Sensing of Environment **215**: 217-227.

Uudeberg, K., A. Aavaste, K.-L. Kõks, A. Ansper, M. Uusõue, K. Kangro, I. Ansko, M. Ligi, K. Toming and A. Reinart (2020). Optical water type guided approach to estimate optical water quality parameters. Remote Sensing **12**(6): 931.

Werther, M., D. Odermatt, S. G. Simis, D. Gurlin, M. K. Lehmann, T. Kutser, R. Gupana, A. Varley, P. D. Hunter and A. N. J. R. S. o. E. Tyler (2022). A Bayesian approach for remote sensing of chlorophyll-a and associated retrieval uncertainty in oligotrophic and mesotrophic lakes. **283**: 113295.

6 Lake Ice cover – LIC

6.1 Candidate algorithms for LIC

The candidate algorithm remains the random forest (RF) classifier and the development plan therefore focusses on improvements to the classification accuracy.

As an ensemble approach, RF integrates decision trees developed by bagging samples to improve the limitations of the single-tree structure (Breiman, 2001). The bagging creates several subsets randomly from training samples with replacement (i.e. a sample can be collected several times in the same subset whereas other samples are probably not selected in this subset). Subsequently, each data subset is used to train a decision tree. For building a single tree, a random sample with several variables is chosen as split candidates from all variables. The number of variables available to a split is one of key RF hyperparameters, denoted as mtry. For the whole RF model, the number of trees (ntree) is defined a priori to develop various independent classifier outputs. The final class of each unknown sample is assigned by the majority vote of all outputs from the trees.

RF has been found to outperform threshold-based approaches (e.g., NASA Snow product), two other machine learning algorithms (multinomial logistic regression, MLR, and support vector machine, SVM) and to provide comparable results to gradient boosting trees (GBT) for lake ice cover, open water and cloud classification (Wu et al., 2021). Training, testing and validation of the MLR, SVM, GBT and RF algorithms from 17 lakes and ice seasons across the northern hemisphere found that RF with a combination of visible, near infrared, and mid infrared bands was the best choice for LIC product generation; more specifically, MODIS Terra/Aqua Level 1B calibrated radiances product (MOD02/MYD02), Collection 6.1 (TOA reflectance data) stored in two separate files as a function of spatial resolution: MOD02QKM/MYD02QKM (250 m, bands 1-2) and MOD02HKM/MYD02HKM (500 m, bands: 3-4, 6-7). While RF and GBT provided similar results following a comprehensive accuracy assessment (cross validation (CV): random k-fold as well as spatial and temporal CV), the former was selected for LIC product generation since it was determined to be less sensitive to the to the choice of hyperparameters necessary for classification compared to GBT, MLR and SVM. High overall accuracy (>95%) has been achieved with the RF classifier in both spatial and temporal transferability assessments (Wu et al., 2021).

6.2 Future improvements for LIC

CRDP v3.0 addresses previously identified issues due to highly turbid lakes and thin cloud/wildfire smoke by adding a temperature filter which corrects ice retrievals using thermal band 31 from the MODIS product. Flags added to the product provide clarity for product generation as well as quality through addition of random forest uncertainty values (Saberi et al., 2025). However, as with any lake product generated from optical data, the presence of clouds as well as extensive cloud cover periods and low solar illumination angles, particularly during the fall freeze-up at high latitudes, introduce classification errors and limit the retrieval of open water and ice cover for many days of the year. Additionally, due to overlap in temperature between water and blue ice classes confusion persists during break-up. .Also, no retrieval can be performed when the solar zenith angle is >85 degrees; a limitation due to the use of MODIS shortwave bands that record very low surface reflectance during ice formation late fall and wintertime.

Given the above limitations, future improvements of the RF classifier and its related processing chain leading to the release of CRDP v4.0 will include: .

1. Addition of new sensors/data into the processing chain such as Sentinel-3 to provide further details on lake conditions.

2. Integration of AI/DL techniques to fill in gaps in the optical data to perform gap-filling/cloud removal during the initial processing phase (for example, The Pretrained Remote Sensing Transformer (Presto) (Tseng et al., 2024).
3. Improvements on the representation of uncertainty and the addition of aleatoric and systematic uncertainty estimates to the LIC product.
4. Continued improvements in identification of ice/water confusion during spring break up

6.3 LIC References

Breiman, L. (2001). Random forests. *Machine Learning*, 45(1), 5–32. doi:10.1023/A:1010933404324.

Saberi, N., C.R. Duguay, E. Hüllermeier, K.A. Scott, and M. H. Shaker (In preparation). Uncertainty estimation of lake ice cover maps from a random forest classifier using MODIS TOA reflectance data.

Wu, Y., Duguay, C.R. & Xu, L. (2021). Assessment of machine learning classifiers for global lake ice cover mapping from MODIS TOA reflectance data. *Remote Sensing of Environment*, 253, 112206, doi: 10.1016/j.rse.2020.112206.

7 Lake Ice Thickness- LIT

7.1 Candidate algorithms for LIT

The number of studies investigating the potential of satellite remote sensing data for the estimation of LIT has been limited to date. Kang et al. (2010) first showed brightness temperature (Tb) measurements from the Advanced Microwave Scanning Radiometer for EOS (AMSR-E) at 18.7 GHz frequency (V polarization) to be highly sensitive (R2 = 0.91) to the seasonal evolution of ice thickness on Great Bear Lake (GBL) and Great Slave Lake (GSL), Canada. Based on this finding, Kang et al. (2014) proposed empirical (linear regression) equations to estimate LIT for the two lakes using 18.7 GHz V-pol data (2002-2009), achieving a mean bias error (MBE) of 0.06 m and root mean square error (RMSE) of 0.19 m when compared to in situ measurements. Surface temperature observations of snow-covered lake ice from the Moderate Resolution Imaging Spectroradiometer (MODIS) have also been assessed for the estimation of LIT. Using heat balance terms and snow depth derived from the Canadian Lake Ice Model (CLIMo, Duguay et al. 2003), Kheyrollah et al. (2017) retrieved ice thicknesses up to ~ 1.2 m from MODIS (2002-2014) with an RMSE of 0.17 m and MBE of 0.07 m when comparing LIT values from single pixels (1 km x 1 km) to those from close by near-shore field measurements collected on GSL and Baker Lake, Canada. Beckers et al. 2017 analyzed waveforms from CryoSat2 (CS2) Ku-band synthetic aperture radar (SAR) altimetry for the estimation of LIT on the Great Bear Lake and Great Slave Lake. By exploiting the increasing distance between peak radar returns from the snow-ice and ice-water interfaces on the leading edge of waveforms with ice growth, the authors estimated ice thickness empirically with RMSE < 0.33 m when compared to in situ measurements from the same near-shore location on GSL as in previous investigations.

While data from CS2 show strong potential for the retrieval of LIT, the drifting orbit of the satellite makes it difficult to build a geographically precise time series of LIT measurements (i.e., repeated along the same tracks over the lifetime of the satellite) required for climate monitoring. Also, the LIT retracker algorithm developed in Beckers et al. (2017) relies on the empirical thresholding of the radar waveforms that is hard to generalize to follow the LIT evolution, in particular at the seasonal transitions, and can lead to biases and sub-optimal LIT estimates. More recent studies, e.g., Shu et al. (2020), Yang et al. (2021), have estimated LIT with radar altimetry data, more specifically from Sentinel-3 and Jason-3 missions, in the context of lake water level analysis, as the presence of lake ice has been shown to introduce a bias on winter water level measurements. These studies also used empirical methods based on already existing retrackers that are not specifically designed for the estimation of LIT.

To overcome the abovementioned limitations, Mangilli et al. (2022) developed a novel physically-based retracking algorithm, the LRM_LIT retracker, founded on the exploitation of the Ku band radar waveforms data in Low Resolution Mode (LRM) data specifically tailored for the retrieval of LIT. The advantage of a physically-based and analytical retracker is that it does not rely on empirical or by-hand settings, allowing to derive robust and continuous LIT estimates over different target lakes and LRM radar altimetry missions, making the LRM_LIT algorithm the suitable tool to build robust and long LIT timeseries for climate monitoring. The LRM_LIT retacker is the algorithm currently being implemented in the lakes_cci LIT processor.

7.2 Future improvements for LIT

The LIT analysis currently done for Phase2 is based on the LRM_LIT algorithm Mangilli et al (2022) (developed in Phase 1), tailored to detect the LIT signature on the Low Resolution Mode (LRM) Ku band waveforms. While this method provides with a significant improvement with respect to current LIT constraints, the accuracy of the LIT retrievals could be further improved by performing the LIT analysis with Ku radar waveform data at higher resolution, namely, UnFocused (UF) SAR and FullyFocused (FF) SAR data. This would imply changing the LIT analytical model as the SAR waveforms and the associated LIT signature over iced covered lake are different from the Low Resolution Mode (LRM) waveforms. An

R&D study on the development and validation of the analytical based LIT retracker for SAR (UF and FF) data has been carried on within the S6JTEX ESA project and the results published in Mangilli et al. (2024). Based on these improvements, the analysis of SAR data for LIT analysis could be timely to be considered for future improvement of the CCI-Lakes LIT products.

7.3 LIT References

K.-K. Kang, C. R. Duguay, S. E. L. Howell, C. Derksen, and R. Kelly, Sensitivity of AMSR-E brightness temperatures to the seasonal evolution of lake ice thickness, IEEE Geoscience and Remote Sensing Letters, vol. 7, no. 4, pp. 751–755, 2010.

K.-K. Kang, C. Duguay, J. Lemmetyinen, and Y. Gel, Estimation of ice thickness on large northern lakes from AMSR-E brightness temperature measurements, Remote Sensing of Environment, vol. 150, pp. 1–19, 2014

H. Kheyrollah Pour, C. R. Duguay, K. A. Scott, and K.- K. Kang, Improvement of Lake Ice Thickness Retrieval From MODIS Satellite Data Using a Thermodynamic Model, IEEE Transactions on Geoscience and Remote Sensing, vol. 55, no. 10, pp. 5956–5965, 2017

Zakharova, E., S. Agafonova, C. Duguay, N. Frolova, and A. Kouraev, 2021. River ice phenology and thickness from satellite altimetry. Potential for climate studies and ice bridge road operation. *The Cryosphere*, 15: 5387-5407, https://doi.org/10.5194/tc-15-5387-2021

J. F. Beckers, J. Alec Casey, and C. Haas, Retrievals of lake ice thickness from Great Slave Lake and Great Bear Lake using CryoSat-2, IEEE Transactions on Geoscience and Remote Sensing, vol. 55, no. 7, pp. 3708–3720, 2017

S. Shu, H. Liu, R. A. Beck, F. Frappart, J. Korhonen, M. Xu, B. Yang, K. M. Hinkel, Y. Huang, and B. Yu, Analysis of Sentinel-3 SAR altimetry waveform retracking algorithms for deriving temporally consistent water levels over ice-covered lakes, Remote Sensing of Environment, vol. 239, p. 111643, 2020

Y. Yang, P. Moore, Z. Li, and F. Li, Lake Level Change From Satellite Altimetry Over Seasonally Ice-Covered Lakes in the Mackenzie River Basin, IEEE Transactions on Geoscience and Remote Sensing, vol. 59, no. 10, pp. 8143–8152, 2021

A. Mangilli, P. Thibaut, C. R. Duguay and J. Murfitt, A New Approach for the Estimation of Lake Ice Thickness From Conventional Radar Altimetry, in IEEE Transactions on Geoscience and Remote Sensing, vol. 60, pp. 1-15, 2022, Art no. 4305515 https://doi.org/10.1109/TGRS.2022.3197109

Mangilli, A.; Duguay, C.R.; Murfitt, J.; Moreau, T.; Amraoui, S.; Mugunthan, J.S.; Thibaut, P.; Donlon, C. Improving the Estimation of Lake Ice Thickness with High-Resolution Radar Altimetry Data. Remote Sens. 2024, 16, 2510. https://doi.org/10.3390/rs16142510

8 Lake Storage Change - LSC

8.1 Candidate algorithms for LSC

In the proposed algorithm, the first step is to check the surface area variability of the lake to distinguish varying and unvarying lakes. This information determines how lake storage change will be retrieved. If the lake to monitor is considered to be varying surface-wise, an estimation of the hypsometric curve (through parametric estimation with polynomial model) from height and surfaces time series is done. The LSC is extracted by the integration of this curve. If the lake is unvarying surface-wise, the LSC is directly computed from the mean area of the lake and height time series with the basic volume formula (which is a volume-to-surface height relationship, see Figure 3).

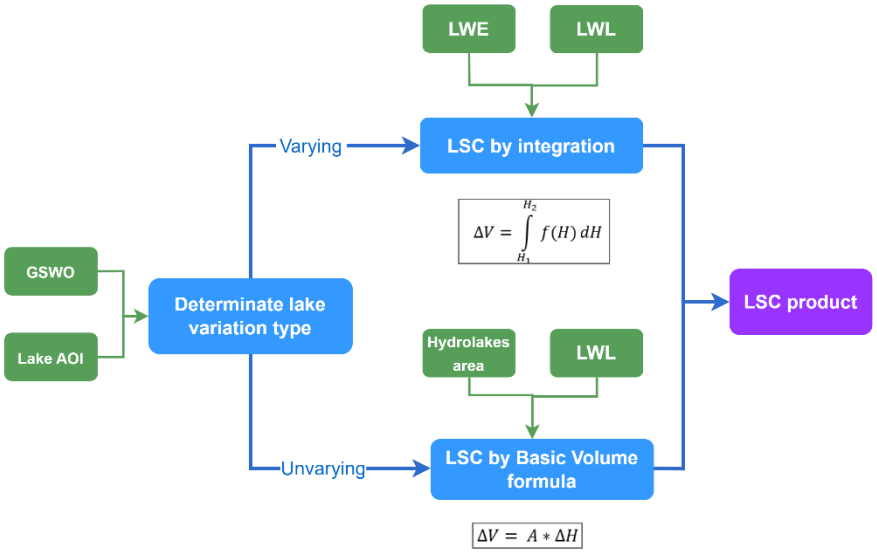

Figure 3: LSC estimation process overview

In the absence of altitude time-series data for both type of lakes, a complementary method has been developed to reconstruct altitude time series, only suitable for surface varying lakes. The use of precise water surfaces is then the starting point to estimate water level, from the lake contour projected on a Digital Elevation Model (DEM). This way, both height and surface are retrieved at the same time, which allows the direct estimation of the hypsometric curve, and uncertainties in the estimate are propagated from the accuracy of the DEM as well as the area estimate.

8.2 Future improvements for LSC

At the initialization of the LSC estimation, we determine whether the lake area is varying surface-wise or not, within a threshold variability of 5%. This threshold could be refined and adapted according to the size of the considered water body to lower the error made on the LSC estimate.

When the lake height time series is not available, we propose to estimate these heights from a DEM when possible. This method is relevant because it increases data density, particularly over time. However, this estimation is subject to manual processing precision, which would require more attention if it were to be automated.

The integration of future sensors such as SWOT will make it possible to provide denser LSC time series.

Finally, a methodology has been proposed for estimating a quality flag, but this method has not yet been automated or applied.

8.3 LSC References

Crétaux, J.-F., Abarca-del-Río, R., Bergé-Nguyen, M., Arsen, A., Drolon, V., Clos, G., & Maisongrande, P. (2016). Lake Volume Monitoring from Space. Surveys in Geophysics, 37(2), 269–305. https://doi.org/10.1007/s10712-016-9362-6

Magome, J., Ishidara, H., & Takeuchi, K. (2003). Method for satellite monitoringof water storage in reservoirs for efficient regional water management. IAHS Publ. no.281, pp.303-310.

Messager, M. L., Lehner, B., Grill, G., Nedeva, I., & Schmitt, O. (2016). Estimating the volume and age of water stored in global lakes using a geo-statistical approach. Nature Communications, 7(1), 13603. https://doi.org/10.1038/ncomms13603

Pekel, J.-F., Cottam, A., Gorelick, N., & Belward, A. S. (2016). High-resolution mapping of global surface water and its long-term changes. Nature, 540(7633), 418–422. https://doi.org/10.1038/nature20584

Appendix A - List of Acronyms

AATSR	Advanced Along Track Scanning Radiometer
AATSR	Advanced Along Track Scanning Radiometer
AERONET-OC	Aerosol Robotic NETwork – Ocean Color
AMI	Active Microwave Instrument
AMSR-E	Advanced Microwave Scanning Radiometer for EOS
APP	Alternating Polarization mode Precision
ASAR	Advanced Synthetic Aperture Radar
ASLO	Association for the Sciences of Limnology and Oceanography
ATBD	Algorithm Theoretical Basis Document
ATSR	Along Track Scanning Radiometer
AVHRR	Advanced very-high-resolution radiometer
BAMS	Bulletin of the American Meteorological Society
BC	Brockman Consult
C3S	Copernicus Climate Change Service
CCI	Climate Change Initiative
CDR	Climate Data Record
CDOM	Coloured Dissolved Organic Matter
CEDA	Centre for Environmental Data Archival
CEMS	Centre for Environmental Monitoring from Space
CEOS	Committee on Earth Observation Satellites
CGLOPS	Copernicus Global Land Operation Service
CIS	Canadian Ice Service
CLS	Collecte Localisation Satellite
CMEMS	Copernicus Marine Environment Monitoring Service
CMUG	Climate Modelling User Group
CNES	Centre national d'études spatiales
CNR	National Research Council of Italy
CORALS	Climate Oriented Record of Altimetry and Sea-Level
CPD	Communication Plan Document
CR	Cardinal Requirement
CRG	Climate Research Group
CSWG	Climate Science Working Group
CTOH	Center for Topographic studies of the Ocean and Hydrosphere
DOC	Dissolved Organic Carbon
DUE	Data User Element
ECMWF	European Centre for Medium-Range Weather Forecasts
ECV	Essential Climate Variable
ELLS-IAGRL	European Large Lakes Symposium-International Association for Great Lakes Research
ENVISAT	Environmental Satellite
EO	Earth Observation
EOMORES	Earth Observation-based Services for Monitoring and Reporting of Ecological Status
ERS	European Remote-Sensing Satellite
ESA	European Space Agency
ESRIN	European Space Research Institute
ETM+	Enhanced Thematic Mapper Plus
EU	European Union
EUMETSAT	European Organisation for the Exploitation of Meteorological Satellites
FAQ	Frequently Asked Questions
FCDR	Fundamental Climate Data Record

FIDUCEO	Fidelity and Uncertainty in Climate data records from Earth Observations
FP7	Seventh Framework Programme
GAC	Global Area Coverage
GCOS	Global Climate Observing System
GEMS/Water	Global Environment Monitoring System for freshwater
GEO	Group on Earth Observations
GEWEX	Global Energy and Water Exchanges
GloboLakes	Global Observatory of Lake Responses to Environmental Change
GLOPS	Copernicus Global Land Service
GTN-H	Global Terrestrial Network – Hydrology
GTN-L	Global Terrestrial Network – Lakes
H2020	Horizon 2020
HYDROLARE	International Data Centre on Hydrology of Lakes and Reservoirs
ILEC	International Lake Environment Committee
INFORM	Index for Risk Management
IPCC	Intergovernmental Panel on Climate Change
ISC	International Science Council
ISO	International Organization for Standardization
ISRO	Indian Space Research Organisation
JRC	Joint Research Centre
KPI	Key Performance Indicators
LEGOS	Laboratoire d'Etudes en Géophysique et Océanographie Spatiales
LIC	Lake Ice Cover
LIT	Lake Ice Thickness
LSC	Lake Storage Change
LSWT	Lake Surface Water Temperature
LWE	Lake Water Extent
LWL	Lake Water Level
LWLR	Lake Water Leaving Reflectance
MERIS	MEdium Resolution Imaging Spectrometer
MGDR	Merged Geophysical Data Record
MODIS	Moderate Resolution Imaging Spectroradiometer
MSI	MultiSpectral Instrument
MSS	MultiSpectral Scanner
NASA	National Aeronautics and Space Administration
NERC	Natural Environment Research Council
NetCDF	Network Common Data Form
NOAA	National Oceanic and Atmospheric Administration
NSERC	Natural Sciences and Engineering Research Council
NSIDC	National Snow & Ice Data Center
NTU	Nephelometric Turbidity Unit
NWP	Numerical Weather Prediction
OLCI	Ocean and Land Colour Instrument
OLI	Operational Land Imager
OSTST	Ocean Surface Topography Science Team
PML	Plymouth Marine Laboratory
PP	Payment Plan
PRISMA	PRecursore IperSpettrale della Missione Applicativa
Proba	Project for On-Board Autonomy
QSR	Quarterly Status Report
R	Linear Correlation Coefficient
RA	Radar Altimeter
RMSE	Root Mean Square Error

SAF	Satellite Application Facility
SAR	Synthetic Aperture Radar
SeaWIFS	Sea-viewing Wide Field-of-view Sensor
SIL	International Society of Limnology
SLSTR	Sea and Land Surface Temperature Radiometer
SoW	Statement of Work
SPONGE	SPaceborne Observations to Nourish the GEMS
SRD	System Requirements Document
SSD	System Specification Document
SST	Sea Surface Temperature
STSE	Support To Science Element
SWOT	Surface Water and Ocean Topography
TAPAS	Tools for Assessment and Planning of Aquaculture Sustainability
TB	Brightness Temperature
TM	Thematic Mapper
TOA	Top Of Atmosphere
TR	Technical Requirement
UNEP	United Nations Environment Programme
UoR	University of Reading
UoS	University of Stirling
US	United States
VIIRS	Visible Infrared Imaging Radiometer Suite
WCRP	World Climate Research Program
WHYCOS	World Hydrological Cycle Observing Systems
WMO	World Meteorological Organization
WP	Work Package